Proceedings World Geothermal Congress 2020+1
Reykjavik, Iceland, April - October 2021

Characterization and efficiency of intermediate cap rock by using XRD and SEM-EDS from the well Glc-1, in Asal-rift geothermal field, Djibouti.

Mohamed Abdillahi Aden[1, 2], Koichiro Watanabe[2], Thomas Tindell[2]

[1]Office Djiboutien de Développement de l'Energie Géothermique (Djibouti)
[2]Kyushu University (Japan)

medabdillahi@mine.kyushu-u.ac.jp

Keywords: Cap-rock, X-ray diffraction, SEM-EDS, Mixed layer chlorite/smectite, Asal-rift Geothermal.

ABSTRACT

This paper reports the results of X-ray diffraction mineralogical studies of the clay-rich from shallow cap-rock. The study area (Asal-field) is one of the most geothermally interesting and tectonically active structures in Djibouti. The X-ray diffraction data were treated using decomposition methods and the peaks identified were performed the investigation cap rocks of the geothermal system developed above of the intermediate reservoir. The additionally Scanning electron microscope (SEM) to this study is to enhances our knowledge and understanding fluid rock interaction in geothermal system, in order to assess the effectiveness and degree of interaction with fluid. The Scanning electron microscope (SEM) is uniquely suited for studying clays because it affords a magnified, three dimensional view to better understand the morphology and detailed information nano to micron scale scale information on crystal-crystal relationships. This clay cap deposit Pleistocene epoch is located between 375m to 421m from the well Glc-1. The upper part is composed of brown to red brown clay; the lower part is composed of grey clay with a plastic tendency. These two levels exits only Gale le Coma area but it is disappear to the northeastern, according from the well Asal-4 and Asal-5. The result of the X-ray diffraction shows quartz, plagioclase, calcite, smectite, Chlorite and interstratified mixed layer chlorite/smectite. The Chemical result of major oxides acquired from SEM-EDS analyses show that the changes in Al and Si which are the main actors in the conversion of smectite to chlorite, do not gradually increase or decrease. SEM imagery also reveals crystal-clay relationship which are important as in some setting clays attach to an alter crystal surfaces which influence permeability and rock strength. Maximum paleo-temperatures higher than 100°C are indicating hot fluid migration from the intermediate reservoir to surface.

1. INTRODUCTION

Clay minerals are widespread alteration products in most of active and fossil geothermal systems and, during the last thirty five years, the availability of these minerals which record in their crystal proprieties the hydrothermal history of the geothermal systems has been intensely investigated (Mas et al., 2006). Many studies have considered both the sequential distribution form smectite to chlorite conversion (Inoue & Utada, 1991; Meng et al., 2018; Robinson & Santana De Zamora, 1999; Son, Yoshimura, & Fukasawa, 2001; Utada, 1984). The characterization of geothermal systems that may dominantly contribute to the maintenance of enthalpy and temperature, usually the cap rock efficiency is mainly evaluated by thickness, thermal alteration and integrity determination but can be affected and reduced by fracturing related to folding. The sequential smectite to chlorite via mixed layer minerals chlorite/smectite (C/S) has been documented in low-temperature environments and is commonly associated with burial diagenesis and hydrothermal alteration. Smectite and chlorite crystallize under neutral pH conditions developing the clay cap zone that usually limits the geothermal reservoir (Vazquez, Bauluz, Nieto, & Morata, 2016). In the present work we extend our investigations in an area located SE of Asal-rift geothermal field (See fig.1), where there is no surface evidence of major geothermal manifestations. The aim of this study is to understand the clay mineral transformation occurring in the shallow caprock reacting with a thermal fluid. Clay minerals were extracted from drill cutting sample (Glc-1 well) and were characterized by a set of techniques including X-ray diffraction, scanning electron microscopy. This study offers the opportunity to improve the knowledge of the geology of the geothermal reservoir in this field.

2. GEOLOGICAL SETTING

The Asal rift is the first emergent segment of the Aden ridge, which propagates westward on land into the Afar depression (Manighetti, King, & Gaudemer, 2001). With a 40km length, whose 15km are emerged, it currently opens at 16mm yr^{-1} in the N40° 5°E direction. This rift is structured by a dense network of fissures and sub-vertical normal faults with throws up to 200m, propagating north-westward (Pinzuti, Mignan, & King, 2010). The evolution of the rift is characterized by the activity of a central volcano, the fiale (Fig.1) which fills the inner floor and conceals previous faults with large volumes of basalt lava flows. Around 50 to 20ky, magmatic activity decrease and the whole successive basalt lava flows that structure the fiale volcano become gradually

offset by normal fault (The latest magmatic episode Ardoukoba (Fig.1) recorded in the rift corresponds to a seismic-volcanic sequence that occurred in 1978 (Anis Abdallah, Lepine, Robineaull, Ruegg, & Tapponnier, 1979)

Mainly the deposition is basalt and porphyritic basalt with same lacustre sediment. In Asal-rift geothermal, all the fault has same direction NE-SW.

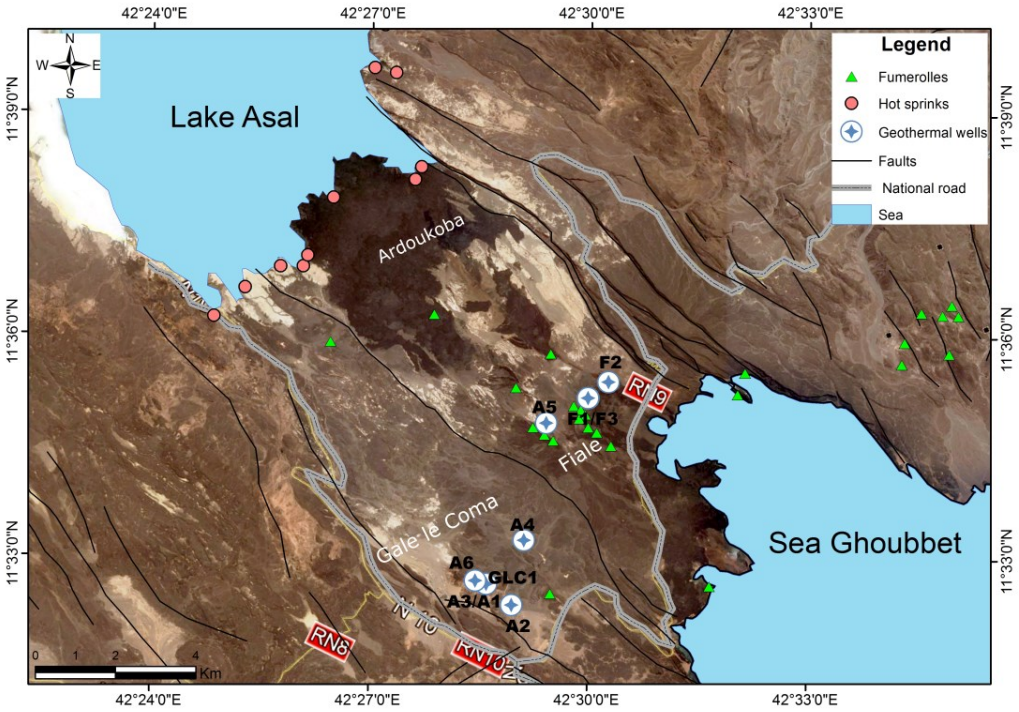

Figure.1: Structural map show the manifestation (hot spring located near the lake Asal and the fumaroles appearin the central part of Asal) and location of the geothermal wells. The study wells (Glc-1) located Gale le Coma SE of Asal (M. Aden, 2018)

Geothermal exploration in the Asal-rift (Fig.1) has a proceeded in to the four phases drilling. The first phase, in the 1970s, consisted of geological, geochemical and geophysical surveys conducted in association with the French geological survey (BRGM); they drilled two deep wells Asal-1 (A1) and A2. The second exploration phase occurred in the in the 1980s, following the 1977 rifting episode associated with the Ardoukoba eruption (Fig.1). The Italian consultancy Aquater conducted four deep wells were drilled (A3, A4, A5 and A6). The third phase ODDEG Company (Local Company) with associated Turkish company (PARS) drill one shallow wells Glc-1 with final depth 543m in 2016. The last phase with multi-donors project invest three directionally wells (F1, F2 and 3) in fiale north-eastern part of Asal (Fig.1). All together ten wells were drilled in Asal-rift geothermal. The main purpose drilled Glc-1 was to confirm the intermediate reservoir or shallow reservoir.

2. SAMPLING AND ANALYTICAL METHODS

This study focused on well Glc-1, which was drilled along vertical axis from the surface to final depth 543m (Fig.2). It should noted that the depth values indicated in this paper refer to the drilling depths. We selected 8 sample from intermediate caprock located between 292m to 421m from Glc-1 well to determine hydrothermal alteration, fluid rock interaction and the transformation of smectite to chlorite. We investigate two methods to determine the alteration and qualitative mineralogical composition; XRD analysis and SEM-EDS.

2.1 X-ray diffraction.

The qualitative mineralogical composition of the bulk samples and clay fraction was obtained by X-ray diffraction (XRD).Bulk sample mineralogy was investigated on randomly oriented whole-rock powders. Preparation of air dried, ethylene glycol (EG) saturated, and HCl treatment clay samples followed the methods. X-ray diffraction (XRD) patterns were recorded Rigaku with Cu-Ka radiation (40kV, 40mA) at the laboratory of Kyushu university. The clay were identified by their characteristic reflections in three differently treated XRD patterns (Moore & Reynolds, 1997). Specifically, the characteristic peak of smectite (S) shifted from

14.2 to 16Å after ethylene glycol saturation; the characteristic peaks of Chlorite (Chl) are 14.2Å, 7Å and 3.54Å these peaks did not shift after ethylene glycol saturation. The intensity of the peak chlorite collapsed after acid treatment (HCl). Illite (Ill) was determined by peaks at 10Å, 5Å and 3.33Å and the position of these peaks did not shift after saturation. The presence of irregular mixed layer based on two peaks, with one located between 16 to 14.3 Å peak (d_{001} reflection) of smectite and the 7.2Å peak (d_{002} reflection) of chlorite.

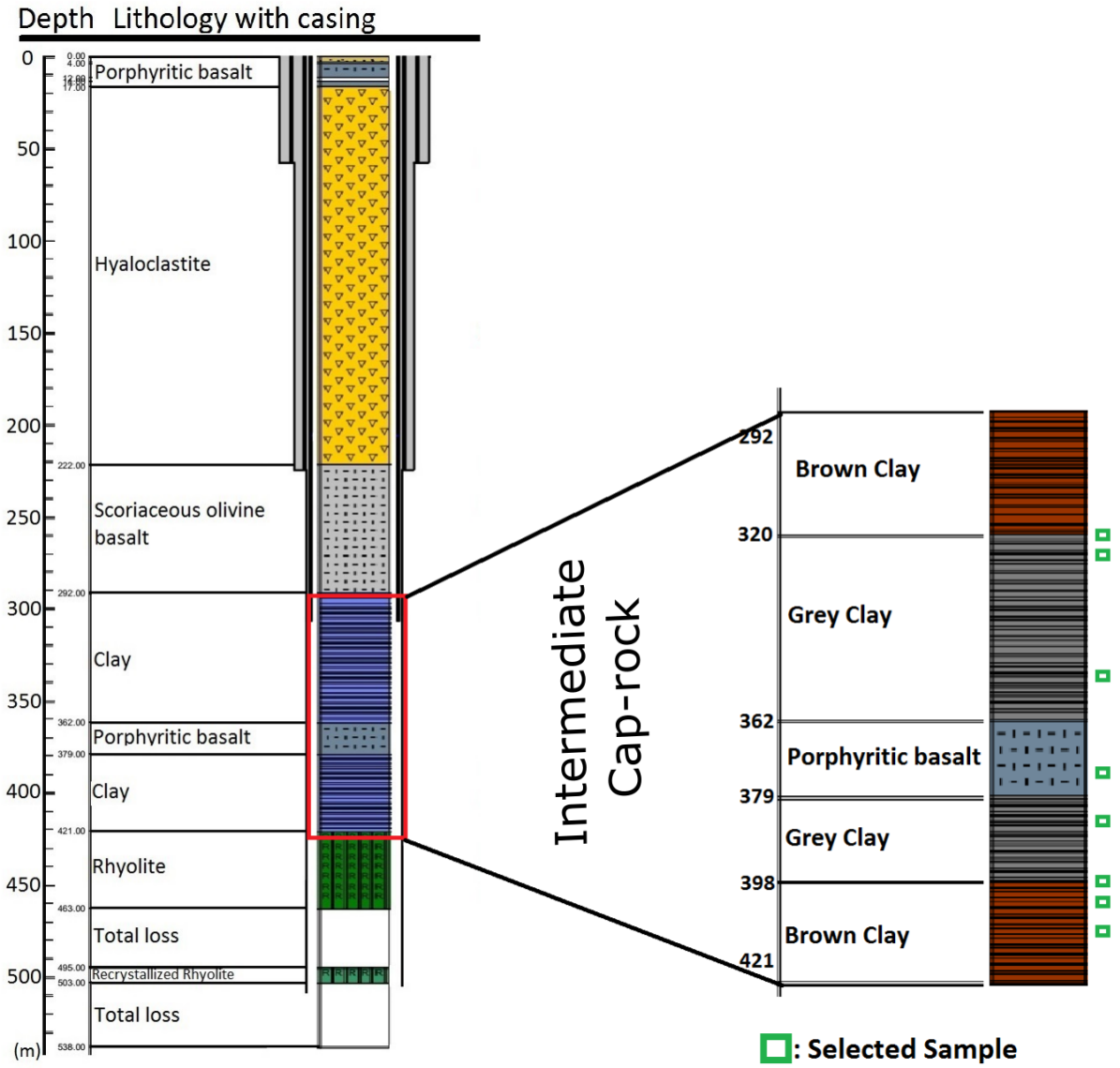

Figure 2: Lithology of the well Glc-1, the intermediate cap-rock located between 292 to 421m which different location of the sample location

In the air dried condition low-charge corrensite (Chlorite/Smectite) has a nominal d(001) of 29.2Å that expands to 31.1Å upon EG solvation.

2.2 Scanning Electron Microscope-Energy dispersive Spectral (SEM-EDS)

Morphological, quantitative and qualitative analyses of the clay samples were carried out using SEM model SU3500. The SEM studies for the mineral analysis of representative samples were conducted in two stages. All the samples were carbon coated in order to make the minerals surface conductive. In the first stage, which was aimed at examining the minerals morphology and identifying their mode of occurrence, crushed carbon stage of the microscopic study was aimed at identifying the mineral phases present within the samples. The quantitative analysis was carried out using the EDX analysis.

3. RESULT

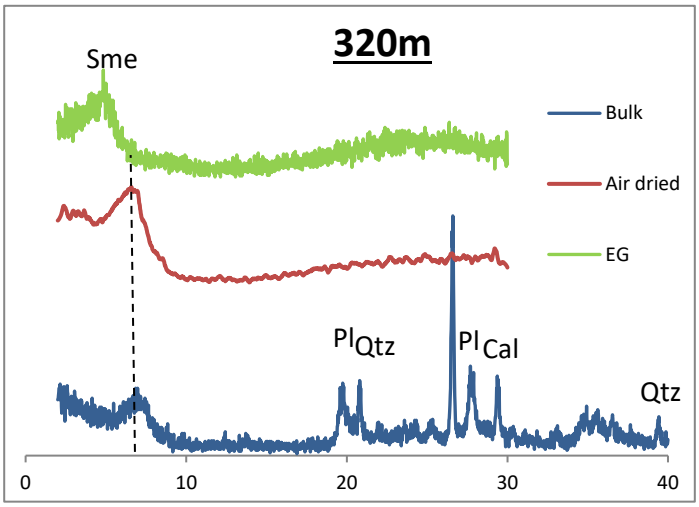
320m
Sme
Bulk
Air dried
EG
Pl
Qtz
Pl
Cal
Qtz
0
10
20
30
40

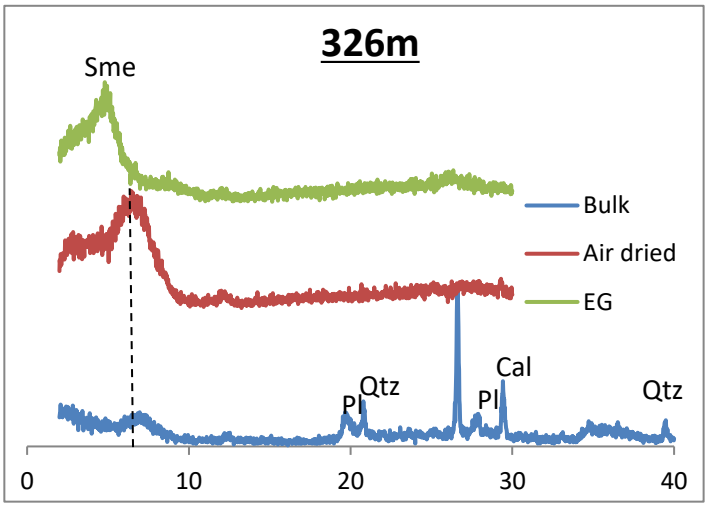
326m
Sme
Bulk
Air dried
EG
Pl
Qtz
Pl
Cal
Qtz
0
10
20
30
40

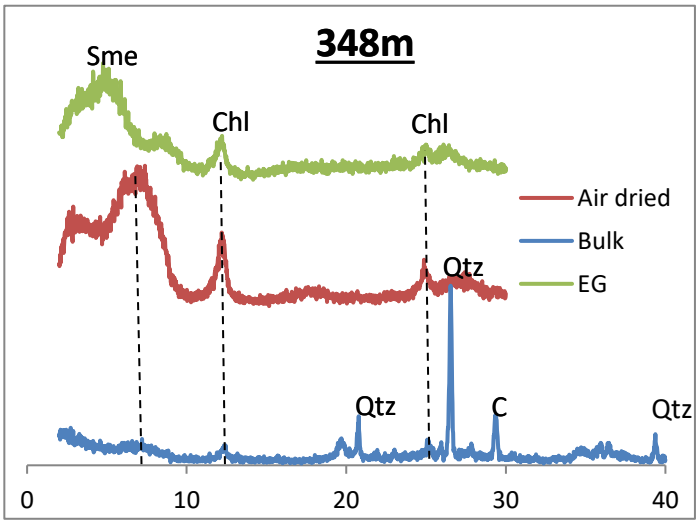
348m
Sme
Chl
Chl
Air dried
Bulk
EG
Qtz
Qtz
C
Qtz
0
10
20
30
40

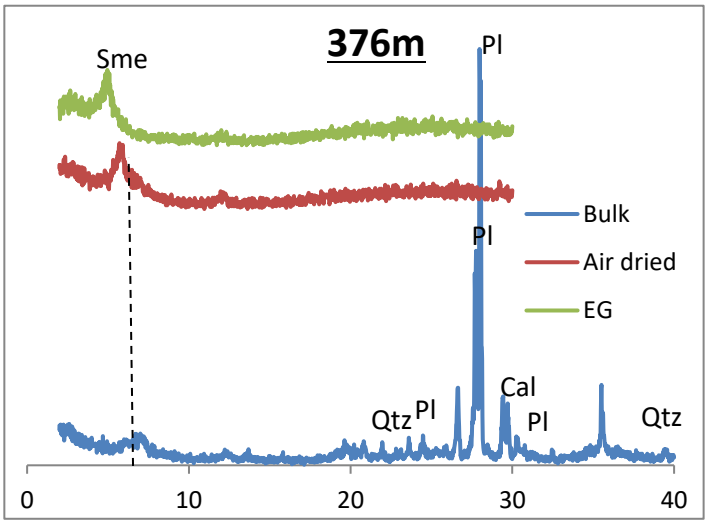
376m
Sme
Pl
Bulk
Air dried
EG
Pl
Cal
Qtz
Pl
Pl
Qtz
0
10
20
30
40

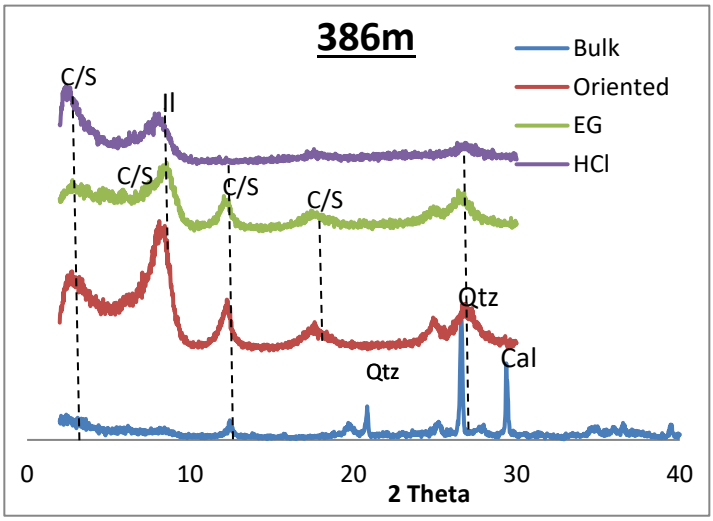
386m
Bulk
Oriented
EG
HCl
C/S
Il
C/S
C/S
C/S
Qtz
Qtz
Cal
0
10
20
30
40
2 Theta

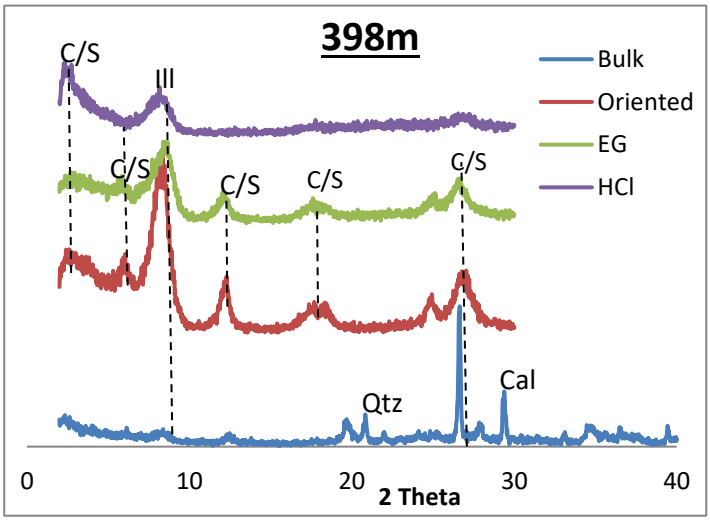
398m
Bulk
Oriented
EG
HCl
C/S
Ill
C/S
C/S
C/S
C/S
Qtz
Cal
0
10
20
30
40
2 Theta

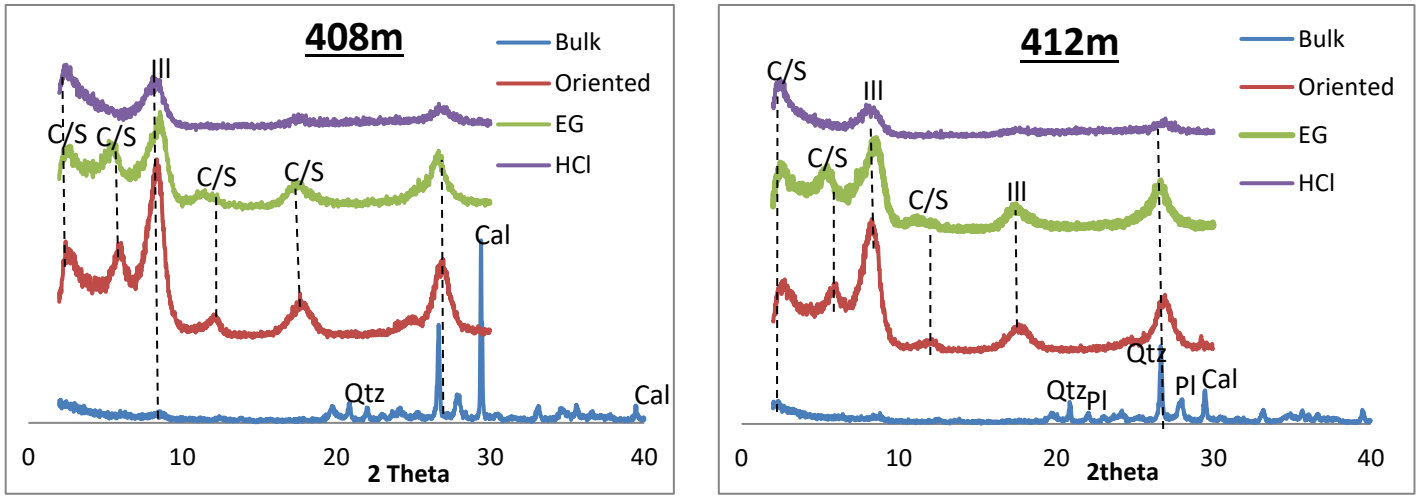

Figure 3: Representative X-ray diffraction patterns of intermediate cap-rock from well Glc-1. 320: Brown coloured claystone; 326: Brown Coloured claystone; 348: the coloured of clay change to black dark; 376: Interlayers altered porphyritic basalt; 386: Grey coloured plastic clay; 398: grey coloured plastic clay; 408: Brown coloured clay; 412: Brown coloured plastic clay. EG: ethylene glycol; Sme: Smectite; Chl: Chlorite; C/S: Chlorite/Smectite; Ill: Illite; Qtz: Quartz; Pl: Plagioclase; Cal: Calcite.

Clays minerals identified in the <2 fraction are shown in table 1. Smectite, illite, Chlorite and interstratified chlorite/smectite are the clay phases identified in the sample. C/S mixed layers have been identified by comparing the air dried (oriented) and ethylene glycol treated specimen (Fig.3). The alteration products identified from sample 320m, 326m, 376m in (fig.3) are dominated by smectite which is expand up to 18Å after glycoled, in sample 320m and 326m expand up to 17Å and sample 348m expand up to 17.8Å after glycoled. In the sample 348m, small peaks at 7.23Å (002) and 3.58Å (004) indicate minor amounts of chlorite, which is resisted after ethanol glycoled. The XRD pattern of sample 386m to 412m shows a three phase phyllosilicate assemblage of smectite, corrensite and chlorite/smectite. In sample 386m shows the chlorite-swelling chlorite (corrensite) with $d_{(001)}$ 30Å, $d_{(002)}$ 14.5Å and $d_{(003)}$ 7.37Å reflections the best XRD evidence of corrensite whose peak position are indicative of 58% chlorite layers. Corrensite is responsible the transformation from smectite to interstratified mixed layer mineral chlorite/smectite (Murakami, Sato, & Inoue, 1999). The chlorite/smectite mixed layer shown a characteristic clay mineral with $d_{(001)}$ 31Å, $d_{(002)}$ 15.3Å, $d_{(003)}$ 7.2Å $d_{(004)}$ 5.01Å, after the solvation of ethylene glycol the $d_{(002)}$ is expand to 16Å but all the chlorite/smectite mineral collapsed after HCl treatment. Illite was identified with peak major 10Å unfortunately illite resisted all treatment. These result indicated that interstratified chlorite/smectite transformed from smectite to corrensite minerals to ordered interstratified minerals.

Sample drilling depth	T (°C)	Lithology	XRD result after Air dried			
			Smectite	Illite	Chlorite	Chlorite/Smectite
320	60	Brown coloured claystone	▬			
326	63		▬			
348	70	Dark clay	▬			
376	79	Interlayers altered porphyritic basalt	▬		—	
386	82	Grey plastic clay		—		▬
398	86			—		▬
408	90	Brown claystone		—		▬
412	97			—		▬

Table 1: drill hole sampling carried out in Glc-1 well along with clay mineralogy (XRD).

▬ : Abundant — : Moderate.

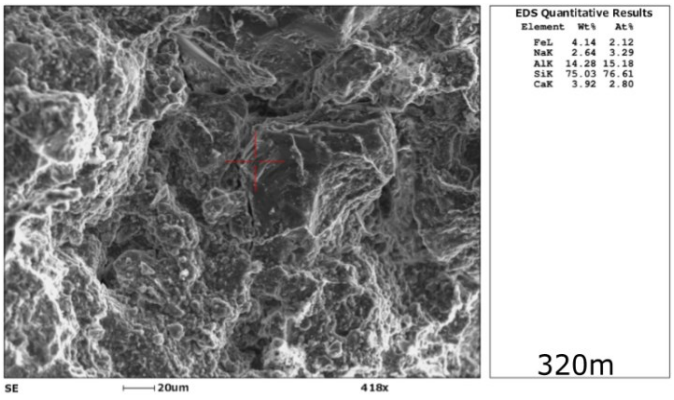
EDS Quantitative Results
Element Wt% At%
FeL 4.14 2.12
NaK 2.64 3.29
AlK 14.28 15.18
SiK 75.03 76.61
CaK 3.92 2.80
320m
SE
20um
418x

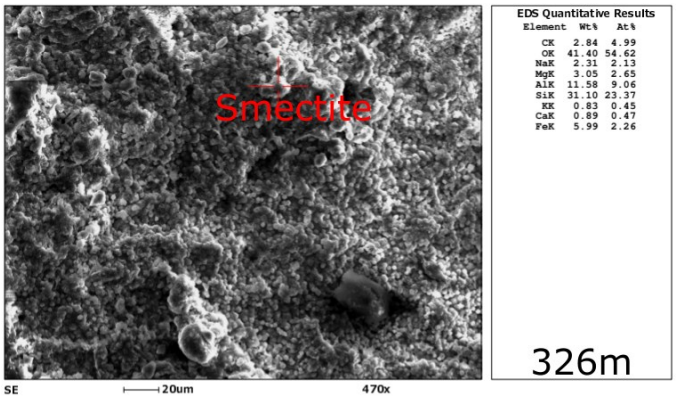
Smectite
EDS Quantitative Results
Element Wt% At%
CK 2.84 4.99
OK 41.40 54.62
NaK 2.31 2.13
MgK 3.05 2.65
AlK 11.58 9.06
SiK 31.10 23.37
KK 0.83 0.45
CaK 0.89 0.47
FeK 5.99 2.26
326m
SE
20um
470x

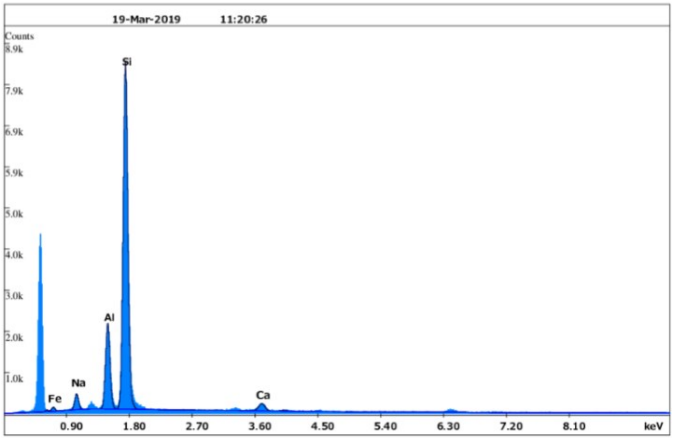
19-Mar-2019 11:20:26
Counts
Si
Al
Na
Fe
Ca
0.90 1.80 2.70 3.60 4.50 5.40 6.30 7.20 8.10 keV

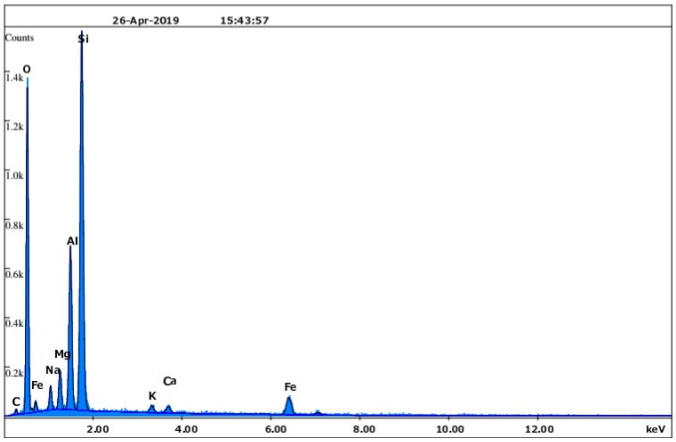
26-Apr-2019 15:43:57
Counts
O
Si
Al
Mg
Na
Fe
C
K
Ca
Fe
2.00 4.00 6.00 8.00 10.00 12.00 keV

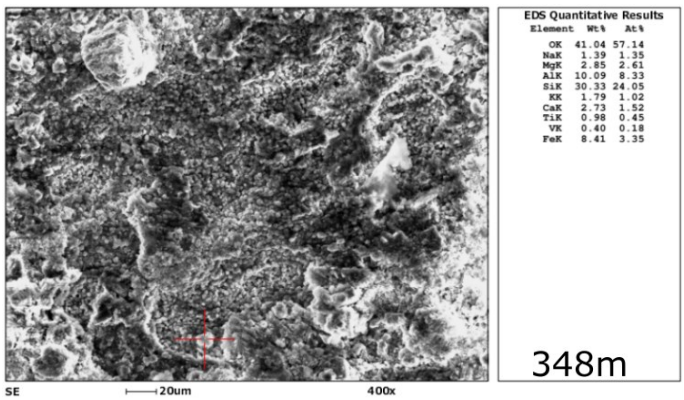
EDS Quantitative Results
Element Wt% At%
OK 41.04 57.14
NaK 1.39 1.35
MgK 2.85 2.61
AlK 10.09 8.33
SiK 30.33 24.05
KK 1.79 1.02
CaK 2.73 1.52
TiK 0.98 0.45
VK 0.40 0.18
FeK 8.41 3.35
348m
SE
20um
400x

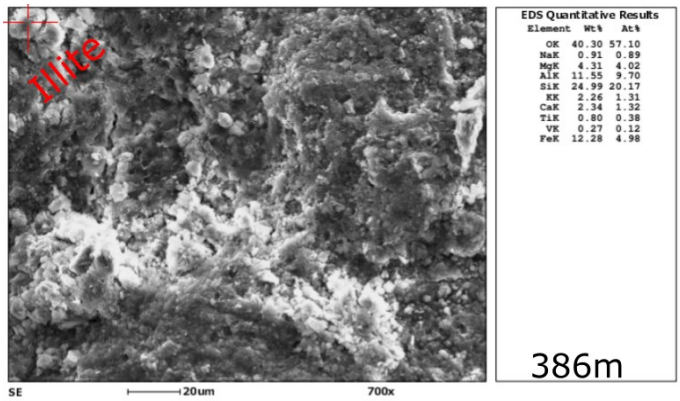
Illite
EDS Quantitative Results
Element Wt% At%
OK 40.30 57.10
NaK 0.91 0.89
MgK 4.31 4.02
AlK 11.55 9.70
SiK 24.99 20.17
KK 2.26 1.31
CaK 2.34 1.32
TiK 0.80 0.38
VK 0.27 0.12
FeK 12.28 4.98
386m
SE
20um
700x

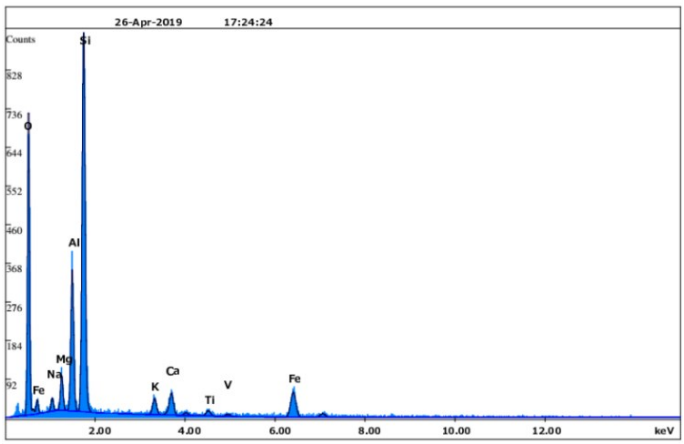
26-Apr-2019 17:24:24
Counts
Si
O
Al
Mg
Na
Fe
K
Ca
Ti
V
Fe
2.00 4.00 6.00 8.00 10.00 12.00 keV

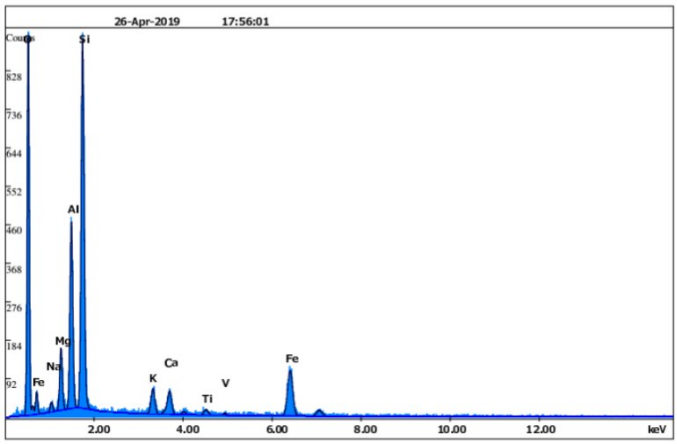
26-Apr-2019 17:56:01
Si
Al
Mg
Na
Fe
K
Ca
Ti
V
Fe
2.00 4.00 6.00 8.00 10.00 12.00 keV

Figure 4: SEM EDS images of core from a geothermal field, sample 320m, 326m and 348m formation of smectite, 386m illite visible on top with increasing the potassium.

SEM provides insight to the subsurface process taking place and altering rocks (Fig.4). The initial formation Smectite (Fig.4, 320) and illite (Fig.4, 386) reveals different clay morphologies and crystal-clay relationship. In sample 320m and 326m shows high Si content, moderate Al and lower Ca and Fe peaks. In sample 398m to 412m clays minerals with a mixed chlorite/smectite composition and two distinctly different crystal degradation. In sample 386m reveals complete dissolution of magnesium it transforms into chlorite/smectite. The SEM-EDS analyses are also used for interpreting the source of the detritic clay mineral and possible deposited of smectite in the sediment sequence. Illite particles usually occur as discrete clasts with angular and irregular outlines, and aggregates of clay particles usually exhibit a typical swirly texture (Song et al., 2018), in sample 386m and 412. The EDS spectra for the sample 408m characterized by strong Si, Al and moderate K peaks, consistent with the chemical composition of illite.

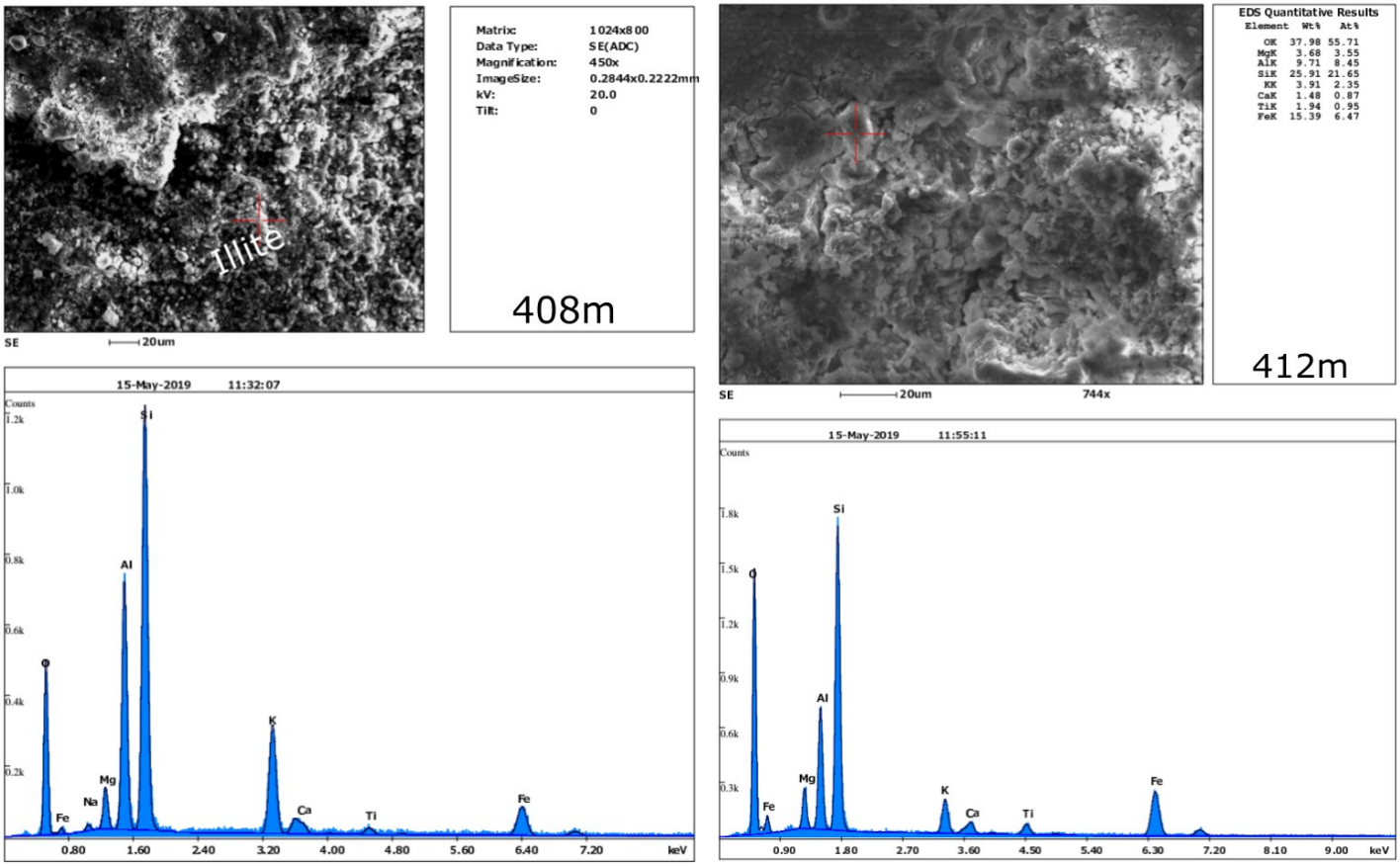

Figure 5: SEM EDS images of core from a geothermal field, sample 408m and 412. The peak K in sample 408 is very strong than sample 412m.

4. DISCUSSION

To investigate the clay mineral transformation in detail, the oriented XRD analysis of raw material experimental samples were exhibited in Fig.3. The first, samples XRD patterns shows same tendency, e.g. a shift of the 001 reflection towards higher angles (from d001=14.82Å to d001=32Å to d001=34Å or 35Å such an evolution can be attributed to the effect of substitution of Al, Na, Si and Fe together with the presence of mixed layer minerals (chlorite/smectite), this substitution was temperature and pressure. Quartz and K-feldspar were also present in the products, as shown in (Fig.3 bulk sample). The intensity of quartz and reflections increased significantly with the increase of temperature and pressure (Cathelineau, 2004). Smectite being the most stable phase in upper levels and evolving to illite and chlorite/smectite in depth. Moreover, the smectite to chlorite sequence has been observed in the sample collected from386m to 412m depth range corresponding to an 82 to 92°C range. The SEM images reveal that the analysed clays are more heterogeneous than the XRD patterns reflect, illustrating the coexistence of different types of clays. On the other hand the combination of SEM-EDS and XRD reveals that. The smectite to chlorite transition has been applied widely as a qualitative measure of metamorphic grade. This has been carried out by documenting the increasing proportion of chlorite layers; or by correlating the progressive changes in the smectite to chlorite transition to well temperature in modern geothermal systems (Robinson & Santana De Zamora, 1999). In the addition the substitution of Si by Al in the tetrahedral positon of chlorite also has been applied widely as a geothermometer (Cathelineau, 1988). As a result, we identified two quality categories for the intermediate

cap rock, 1) Smectite dominate in the above, 2) reacting after temperature increase become mixed layer clay mineral. Cap rocks features by low levels of thermal alteration, low content of illite layers in mixed layers chlorite/smectite.

The conversion of smectite to Chlorite via interstratified mixed layer chlorite/smectite into two steps of reaction according (Utada, and Inoue, 1984); the one which is represented by reaction (a) in (fig.6) is the reaction from smectite to corrensite, the second which is represented by reaction (b) in (fig.6) is that from corrensite to chlorite. In the reaction (a) chlorite layer formed in the smectite layers will be incorporated into the formation of correnstite with advancement of the conversion. A unit of interstratified phase which is composed of one smectite layer (SS) and one corrensite layer (SC) as component layers occurs in the earlier stage of the conversion. The reason is that the corrensite packets early produced in the smectite layers tend to segregate from the parent smectite layers. The chlorite layers in the corrensite packets are likely to tend to segregate from the correnstie layers with advancement of the conversion.

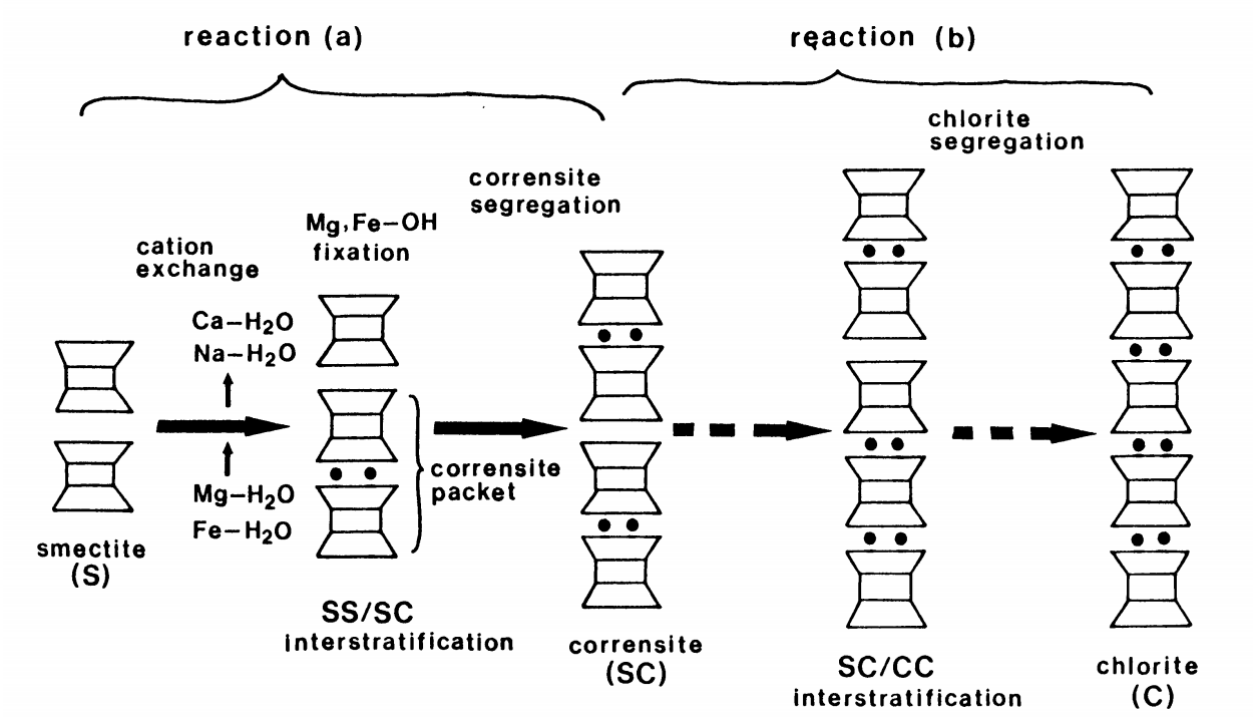

Figure 6: Schematic diagram showing the conversion reaction of smectite to chlorite through intermediate chlorite/smectite. Reaction (a) corresponds to a reaction from smectite to corrensite and reaction (b) from corrensite to chlorite, after (Utada and Inoue, 1984)

5. CONCLUSION

We performed XRD and SEM-EDS investigations of the whole-rock composition and <2micrometer of the sedimentary cap rock of the geothermal system developed in subsurface. This investigation allowed us to recognizing differences in clay minerals assemblages within intermediate cap rock. From our result we infer that the cap rock is effective as indicated by the preservation. In the literature, smectite/chlorite mixed layer minerals are generally considered to be product from smectite with segregate corrensite, when Mg, Fe and Al ions are fixed as hydroxides in the interlayers of trioctahedral smectite, the fixed layer is easily transformed in to chlorite layer because of greater layer charge of trioactahedral smectite.

RECOMMENDATION

Detailed HRTEM to be carried out to showed a wide variety of the microstructures of interstratified chlorite/smectite and EPMA to characterize the chemical composition of the conversion from smectite to chlorite.

REFERENCES

Anis Abdallah, Lepine, J., Robineaull, B., Ruegg, J., & Tapponnier, P. (1979). *articles Relevance of Afar seismicity and volcanism to the mechanics*. *282*(November), 17–23.

Cathelineau, M. (1988). Cation site occupancy in chlorites and illites as a function of temperature. *Clay Minerals*, *23*(4), 471–485. https://doi.org/10.1180/claymin.1988.023.4.13

Cathelineau, M. (2004). *Experimental transformation of Na , Ca-smectite under basic conditions at 150 j C*. *26*, 259–273. https://doi.org/10.1016/j.clay.2003.12.011

Inoue, A., & Utada, M. (1991). Smectite-to-chlorite transformation in thermally metamorphosed volcanoclastic rocks in the Kamikita area, northern Honshu, Japan. *American Mineralogist*, *76*(3–4), 628–640.

M. Aden, Thomas tindell, K. Watanabe. (2018). SUB-SURFACE GEOLOGY OF HYDROTHERMAL ALTERATION AND 3D GEOLOGICAL MODEL OF THE WELLS , GLC-1 , ASAL 3 , 4 and 5 IN ASAL-RIFT. *ARGEO-C7 Conference*, (November), 1–13.

Manighetti, I., King, G. C. P., & Gaudemer, Y. (2001). *Water Volcanoes*. *106*(B7), 13,667-13,696.

Mas, A., Guisseau, D., Patrier Mas, P., Beaufort, D., Genter, A., Sanjuan, B., & Girard, J. P. (2006). Clay minerals related to the hydrothermal activity of the Bouillante geothermal field (Guadeloupe). *Journal of Volcanology and Geothermal Research*, *158*(3–4), 380–400. https://doi.org/10.1016/j.jvolgeores.2006.07.010

Meng, J., Liu, X., Li, B., Zhang, J., Hu, D., Chen, J., & Shi, W. (2018). Conversion reactions from dioctahedral smectite to trioctahedral chlorite and their structural simulations. *Applied Clay Science*, *158*(April), 252–263. https://doi.org/10.1016/j.clay.2018.03.033

Moore, D. M., & Reynolds, R. C. (1997). *X ' Ray Diffraction and the Identification and Analysis of Clay Minerals SECOND EDITION*.

Murakami, T., Sato, T., & Inoue, A. (1999). HRTEM evidence for the process and mechanism of saponite-to-chlorite conversion through corrensite. *American Mineralogist*, *84*(7–8), 1080–1087. https://doi.org/10.2138/am-1999-7-810

Pinzuti, P., Mignan, A., & King, G. C. P. (2010). Surface morphology of active normal faults in hard rock: Implications for the mechanics of the Asal Rift, Djibouti. *Earth and Planetary Science Letters*, *299*(1–2), 169–179. https://doi.org/10.1016/j.epsl.2010.08.032

Robinson, D., & Santana De Zamora, A. (1999). The smectite to chlorite transition in the Chipilapa geothermal system, El Salvador. *American Mineralogist*, *84*(4), 607–619. https://doi.org/10.2138/am-1999-0414

Son, B. K., Yoshimura, T., & Fukasawa, H. (2001). Diagenesis of dioctahedral and trioctahedral smectites from alternating beds in miocene to pleistocene rocks of the Niigata Basin, Japan. *Clays and Clay Minerals*, *49*(4), 333–346. https://doi.org/10.1346/CCMN.2001.0490407

Song, B., Zhang, K., Zhang, L., Ji, J., Hong, H., Wei, Y., … Wang, C. (2018). Qaidam Basin paleosols reflect climate and weathering intensity on the northeastern Tibetan Plateau during the Early Eocene Climatic Optimum. *Palaeogeography, Palaeoclimatology, Palaeoecology*, *512*(December), 6–22. https://doi.org/10.1016/j.palaeo.2018.03.027

Utada, I. and watanabe. (1984). *Conversion of Trioctahedral Smectite To Interstratified Chlorite / Smectite in Pliocene Acidic Pyroclastic Sediments of the Ohyu District , Akita Prefecture , Japan*. *116*, 103–116.

Vazquez, M., Bauluz, B., Nieto, F., & Morata, D. (2016). Illitization sequence controlled by temperature in volcanic geothermal systems: The Tinguiririca geothermal field, Andean Cordillera, Central Chile. *Applied Clay Science*, *134*, 221–234. https://doi.org/10.1016/j.clay.2016.04.011